LA-UR -91-3217

LA-UR--91-3217

DE92 002364

Los Alamos National Laboratory is operated by the University of California for the United States Department of Energy under contract W-7405-ENG-36.

TITLE: Tokamak and RFP Ingition Requirements

AUTHOR(S): Kenneth A. Werley, A-3

SUBMITTED TO: Fourteenth Symposium on Fusion Engineering

DISCLAIMER

Los Alamos Los Alamos National Laboratory
Los Alamos, New Mexico 87545

FORM NO 836 R4
ST NO 2629 5/81

TOKAMAK AND RFP IGNITION REQUIREMENTS

K. A. Werley
Los Alamos National Laboratory, MS F607, Los Alamos, NM 87545

Abstract. A plasma model is applied to calculate numerically transport-confinement ($n\tau_E$) requirements and steady-state operation points for both the reversed field pinch (RFP) and tokamak. The CIT tokamak and RFP ignition conditions are examined. Physics differences between RFP and tokamaks, and their consequences for a DT ignition machine, are discussed. The ignition RFP, compared to a tokamak, has many physics advantages, including ohmic heating to ignition (no need for auxiliary heating systems), higher beta, lower ignition current, less sensitivity of ignition requirements to impurity effects, no hard disruptions (associated with beta or density limits), and successful operation with high radiation fractions ($f_{RAD} \sim 0.95$). These physics advantages, coupled with important engineering advantages associated with lower external magnetic fields, larger aspect ratios, and smaller plasma cross sections translate into significant cost reductions for both ignition and power reactor. The primary drawback of the RFP is the uncertainty that the present confinement scaling will extrapolate to reactor regimes. The 4-MA ZTH was expected to extend the $n\tau_E$ transport scaling data three orders of magnitude above ZT-40M results, and if the present scaling held, to achieve a DT-equivalent scientific energy breakeven, $Q = 1$. A basecase RFP ignition point is identified with a plasma current of 8.1 MA and no auxiliary heating.

1. INTRODUCTION

It has been long realized that reversed field pinches (RFP) have the potential for reaching ignition with ohmic heating alone. Lawson[1] derived a criterion for RFP ignition provided transport and impurity radiation losses are sufficiently small. Even in the earliest RFP reactor (RFPR) studies, the RFP features of ohmic ignition and high beta made it "clear that when RFPR is compared with the tokamak under the same ground rules ...the RFPR could represent a realistic alternative in the continuous development of a fusion power source."[2] The present work applies an impurity model and a transport energy confinement relation based upon experimental results from the international RFP community, to identify RFP ignition requirements and to compare with tokamak ignition requirements. The differences in ignition physics between the RFP and tokamak are also discussed.

Section 2 summarizes the steady-state, 0-D model. The model describes either tokamak or RFP confinement concepts through appropriate changes in the magnetic equilibrium, plasma beta, ohmic heating, and confinement scaling relations. Ignition conditions are discussed in Sec. 3. First, $n\tau_E$ requirements for tokamaks and RFP to achieve high Q ($Q \gtrsim 5$) operating regimes are examined. Next, confinement relations are applied, and both tokamak and RFP ignition requirements are examined and compared.

2. STEADY-STATE, 0-D MODEL

The steady-state model includes ion and electron energy balance; protium, deuterium, tritium, helium-3 and helium-4 (alpha) particle continuity; a specified ionic fraction for a high-Z impurity; charge balance; a plasma beta constraint; and magnetic equilibrium constraints. The 0-D equations are obtained through a radial average over specified plasma profiles. A detailed description of the model equations and the computer codes used to calculate solutions, as well as applications to RFP experimental regimes, can be found in Ref. 3 and 4.

The steady-state, 0-D, ion and electron energy-balance equations include fusion, auxiliary and ohmic heating, electron-ion equipartition, transport, and bremmstrahlung, cyclotron and line radiation. The fractional fusion power deposited in the ions is calculated through a time integral over the slowing down time of the slowing down rate on the ions; zero prompt loss is assumed. Cyclotron radition loss is a function of the effective wall reflectivity for cyclotron radiation, R_{CYC}, which includes the effects of wall reflection and holes in the wall. The fractional auxiliary power going to the ions, f_{AUX_i}, and auxiliary power, P_{AUX}/n^2, must also be specified.

The ohmic heating term is given by $P_{OH} = \int \eta_{\|} J_{\|}^2(r) dV$. Here, $\eta_{\|}$ is the classical parallel electrical resistivity[5], and $J_{\|}(r)$ is the parallel current density profile.

All background ions are assumed to share the same local temperature, $T_i(r)$, and to have a common profile. The total ion density, n, the electron density, n_e, (assuming charge neutrality) and the effective ionic charge, Z_{eff}, are given by summing over the ion species. The average Z and Z^2 of impurity species and the line radiation are calculated based upon the assumption of coronal equilibrium. All ion species are assumed to have the same particle confinement time, τ_p. The values of the fractional composition of the fuel, as well as the ratio of τ_p to τ_{E_e}, must be specified.

The transport energy losses are represented in terms of ion and electron transport energy confinement times. The total transport energy confinement time is given by

$$\tau_E = (nT_i + n_eT_e)/(nT_i/\tau_{E_i} + n_eT_e/\tau_{E_e}) \ . \qquad (1)$$

The ratio of τ_{Ei}/τ_{Ee} must be specified in this model. Goldston[6] scaling is assumed for the tokamak.

$$\tau_E^{tok} = (\tau_{OH}^{-2} + \tau_A^{-2})^{-1/2} \qquad (2)$$

The "ohmic" confinement time, τ_{OH}, is given by the neo-Alcator expression[6] with the ion line density defined by $N = n\pi\kappa a^2$ where κ is the plasma elongation, and the cylindrical safety factor, q_{cyl}, is defined in terms of magnetic equilibrium parameters.

$$n\tau_{OH} = \kappa^{-2} R^{2.04} a^{-2.96} q_{cyl}^{0.5} N^2 \qquad (3)$$

$$q_{cyl} = 5\varepsilon a B/I_\phi \ (0.5 + \kappa^2(0.5 + \delta^2)) \qquad (4)$$

The auxiliary-heating confinement time, τ_A, is also given by Goldston[6], with $H_G = 2$ for H-mode confinement.

$$n\tau_A = H_G 2.84 \times 10^{17} R^{2.5} a^{-2.74} I^2/(T_i + f_eT_e) \qquad (5)$$

The RFP scaling relation is provided by a fit of $n\tau_E$ to experimental data[7] in an analogous fashion as the τ_E fits of DiMarco[8].

$$n\tau_E = C_\tau 3 \times 10^{27} [I_\phi^3 (f_eN)^{-0.5}]^X \qquad (6)$$

The case of $C_x = 3.28$ and $X = 1$ provides a one-parameter fit of international RFP results to Connor-Taylor[9] theoretical scaling. The variable f_e is defined as n_e/n_i.

The fractional beta carried by athermal (hot) fusion products, $f_{\beta H}$, must be specified and is used in defining the plasma beta, β. The toroidal beta is required for the tokamak option, while for the RFP option, poloidal beta is needed. The operating value of β is specified for use in the tokamak option through the Troyon[10] beta-limit constraint, $\beta_T = 0.03 I_\phi/(aB)$. The equilibrium constraints for the tokamak are taken from Peng[11] and provide formulae for I_ϕ/aB as a function of elongation, triangularity, δ, edge safety factor, $\bar{q}$, and the inverse aspect ratio. For the RFP option, the situation is greatly simplified because $B = B_\phi(a)$, so $I_\phi/aB = 5$.

To complete the 0-D description, plasma profiles for density, temperature, and current density are specified using $x \equiv (r/a)^2$ and an exponent of the form $T(x) = T_o(1-x)^{\alpha_T}$. For the tokamak case, $J_\parallel(r)$ is assumed to be $J_\phi(r)$ and $\alpha_J = 1.5\alpha_T$[12]. These assumptions are only used in calculating P_{OH}, which is typically weak for tokamak ignition conditions of interest. For the RFP, an approximate representation of the current density profile is given in Ref. [3]. The $J_\parallel$ profile accounts for the helical path of magnetic field lines resulting from the equivalent magnitude of the poloidal and toroidal fields in the RFP. This factor is crucial for estimating the voltages and ohmic power in the RFP. Approximating the plasma as an elliptical cylinder with flux surfaces of concentric ellipses, profile form factors are calculated for all terms.

Summarizing the model, the plasma continuity equations together with the profile form factors and the magnetic equilibrium constraints, form a complete set of equations for calculating $n\tau_E$. Input parameters include T_i, I_ϕ, magnetic topology, and profile exponents, as well as confinement time ratios, $\frac{\tau_p}{\tau_{E_e}}$ and $\frac{\tau_{E_i}}{\tau_{E_e}}$, high-Z impurity fractions, particle refueling fractions, auxiliary heating information, P_{AUX} and f_{AUX_i}, the fractional beta carried by hot (athermal) fusion products, $f_{\beta H}$, and the cyclotron-radiation wall reflectivity, R_{CYC}. Output includes the fuel and fusion-product particle fractions, the product aB, the beta, the electron temperature, and the $n\tau_E$. Since $n\tau_E$ products are desired, solutions can be obtained without knowledge of absolute particle densities, only fractional densities are required, (e.g., $f_j = n_j/n$). Absolute values of minor radius and magnetic field are also not required.

If additionally the appropriate empirical $n\tau_E$ scaling correlation is provided, the particle density fractions are specified, and the beta specification is dropped, then the model can be used to calculate steady-state operating points. The stability of the operating points to fixed-density and fixed-current perturbations in temperature can also be evaluated. The stability check permits identification of both ignition and stable operating points.

3. RESULTS

3.1. Required $n\tau_E$

The first application of the model does not assume a transport-confinement scaling relation, but rather calculates an $n\tau_E$ value that the actual transport mechanism must allow for a plasma to achieve a steady-state operating point. This transport confinement must balance the energy sources minus the radiation losses, and must be consistent with particle continuity and magnetic equilibrium. These required-$n\tau_E$ values are calculated for a fixed plasma current and a specified beta constraint and are plotted versus ion temperature. Assumptions of the model include $\tau_p/\tau_{E_e} = \tau_{E_i}/\tau_{E_e} = 4$, $\alpha_n = \alpha_T = 1$, $R_{CYC} = 0.8$, and $f_{\beta_H} = 0.17$.

3.1.1. Tokamaks. The required $n\tau_E$ is plotted as dashed curves in Fig. 1 for a DT tokamak plasma with no high-Z ($Z > 2$) impurities. Tokamak specific assumptions include $I_p = 10MA$, $C_T = 0.030$, $\kappa = 0.2$, $\delta = 1.8$, $\epsilon = 0.3704$, $f_{AUX_i} = 0$. The result is independent of plasma minor radius, but if the plasma had a minor radius of $a = 0.45\ m$, the resulting magnetic field would be $B = 10.4T$. These input parameters are for the Compact Ignition Tokamak (CIT) conceptual design point[13]. The $Q_{AUX} = 999$ curve [$Q_{AUX} \equiv P_F/P_{AUX}$] represents the case of negligible auxiliary heating and has typical plasma Q-values of 400-600 [$Q \equiv P_F/(P_{AUX} + P_{OHM}$], thus ohmic heating is negligible. This curve represents ignited plasma conditions, and, since ohmic heating is so small, can only be reached by auxiliary heating. The ignition boundary is defined by where fusion heating is sufficiently strong that a constant-current perturbation in energy, away from a steady operating point, is thermally unstable and would run away. The ignition boundary is approximately given by a Q = 5 curve, where the fusion heating rate equals the other heating terms. This ignition boundary must be achieved to accomplish CIT mission goals of studying alpha-particle physics and operating-point stability under fusion-product-heating dominated conditions. For tokamaks, $Q_{AUX} \simeq Q = 5$, and this curve is also plotted in Fig. 1. These results depend only weakly upon plasma current through ohmic and cyclotron terms, both of which are typically small for ignited DT tokamaks.

3.1.2. RFP. The required $n\tau_E$ for the RFP is also plotted in Fig. 1, including Q = 5 points. The RFP differ from tokamaks in that ohmic heating is sufficiently large that no auxiliary heating is necessary ($Q_{AUX} = \infty$) and $n\tau_E$ requirements depend strongly on current. Thus, if beta remains high and electrical conductivity follows a classical[5] scaling, as in present RFP experiments, then ignition can be achieved by driving modest levels of plasma current. The circles in Fig. 1 represent Q = 5 (near-ignition) points. Note that the tokamak $Q \simeq Q_{AUX} = 5$ curve passes through these circles, demonstrating that the $n\tau_E$ ignition requirement is similar for the RFP and tokamak. This result implies that the differences in equilibrium cause negligible differences in the radiation losses for the near-ignition regime. The major difference between the two devices, then, is that, for the RFP, a continuum of solution points exists between ignition and present experimental conditions without requiring auxiliary

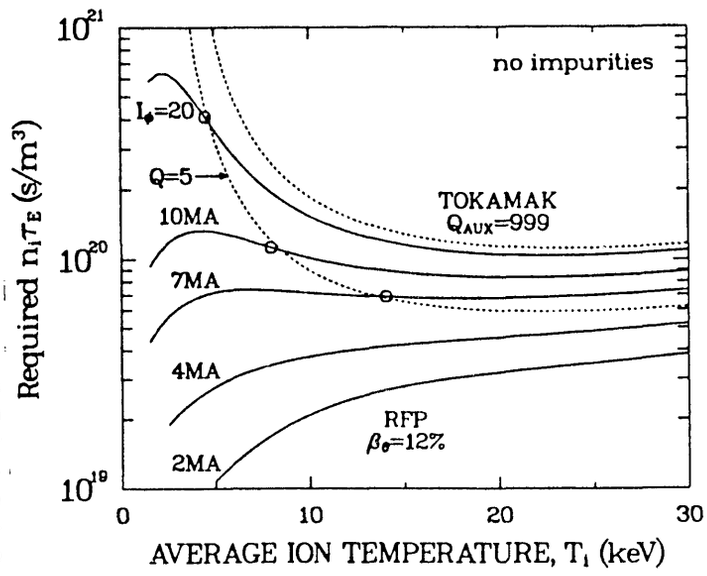

Fig. 1 Required $n\tau_E$ versus ion temperature for a tokamak (dash) and an RFP (solid) with no impurities.

heating systems. Thus, while standard tokamaks must be supplied with extra power to access the "Cordey mountain pass" to achieve ignition, the RFP need only be driven with sufficient plasma current.

The difference in the relative importance of ohmic heating for the RFP and tokamak can be understood by examining the magnitude of the average ohmic power density divided by density squared, $P_{OH}/n^2 = \eta_{\|}(J_{\|}/n)^2$. The n^2 divisor is used because all other terms in the energy balance equation are proportional to n^2, so the ratio, P_{OH}/n^2, can be compared to the rest of the energy balance equation (which is approximately independent of density). If $c_J \equiv J_{\|}/J_{\phi}$, then $J_{\|}/n = c_J I_{\phi}/N$. Using the definition of poloidal beta gives $I_{\phi}/N \sim T/(I_{\phi}\beta_{\theta})$. Major disruptions observed in tokamaks limit the tokamak poloidal beta to larger values than the RFP. Also, tokamaks have $c_J \approx 1$, while RFP have large poloidal and toroidal currents such that $c_J \approx 3$. These two features combine for plasmas of the same toroidal current, and temperature to provide two orders of magnitude larger values of P_{OH}/n^2 for the RFP.

3.2. Tokamak Ignition Regime

Two limiting tokamak transport scaling relations were used to bracket the expected range of available scaling. On the optimistic side, neo-Alcator was chosen, while on the pessimistic side, twice-Goldston L-mode was used [Eqs. (1)-(4)]. Assumptions, except for the scaling, are taken from a more recent CIT design[14], which is larger and has more current and auxiliary heating the CIT conceptual design report[13]. Specific assumptions include $a = 0.64m$, $B = 11T$, $\kappa = 2.0$, $\delta = 0.2$, $\epsilon = 0.3048$, $f_{AUX_i} = 0.2$. Figure 2 contains N *versus* T_i steady-state operating points for an 11 MA tokamak, under neo-Alcator scaling with no line radiation and $Z_{eff} = 1.5$.

The curves in Fig. 2 satisfying $T_i < 3keV$ predominantly balance ohmic heating (plus P_{AUX}) against losses. Even under this idealistic scaling assumption, ohmic heating is insufficient to heat the plasma beyond 2.5 keV. Above 3 keV, the energy sour) is predominantly fusion (plus P_{AUX}). Above a line density of $10^{21}/m$, the loss mechanism is mainly bremmstrahlung radiation, while below $10^{21}/m$, the losses are mainly transport. The space between the ohmic and the fusion curves is a cooling region where losses are greater than sources; a plasma in this region would cool down to the ohmic curve. The space to the right of the fusion-dominated curve is a heating region. For auxiliary heating of $P_{AUX}/n^2 = 3 \times 10^{-42}\ MW\text{-}m^3$ and for CIT conditions, this implies $P_{AUX} = 12.5\ MW$. The Hugill electron density limit for ohmic and ICRH heated, gas-fueled plasmas is also plotted in Fig. 2.

Figure 3 contains the same plot as Fig. 2, except 2% carbon and 0.2% iron, including line radiation, are added to the plasma. The effect of these impurities is to shift the fusion-dominated $P_{AUX} = 0$ curve from $T_i < 5\ keV$ to $T_i > 11\ keV$. Even with $P_{AUX}/n^2 = 5 \times 10^{-41}\ MW\text{-}m^3$, which for a line density of $4 \times 10^{20}/m$ corresponds to $P_{AUX} = 41\ MW$, the plasma is far from ignition. The CIT design value for auxiliary heating is 30 MW. Clearly, successful impurity control is necessary to minimize CIT ignition requirements, and

too many impurities in CIT could prevent ignition. With no line radiation, $I\phi = 11$ MA, and Goldston-H scaling, a maximum value of $Q = 4$ is obtained, and ignition ($Q \simeq 5$) cannot be achieved, even for very large heating, $P_{AUX} \simeq 150\ MW$. This agrees with results of the CIT conceptual design report[13].

3.3. RFP Ignition Regime

The Connor-Taylor scaling relation (based upon a one-parameter fit to the international database) was chosen by the Los Alamos ZTH[15] design team. The approach of the present study extends application of this scaling relation to evaluate the ignition requirements of a next step (after ZTH) device.

To highlight the important role of ohmic heating in the RFP, a calculation was done for the case of no fusion power. All other physics terms were applied, including radiation. Results plotted as a dashed curve in Fig. 4 demonstrate RFP plasmas can achieve high temperatures at relevant line densities by ohmic heating alone. By comparison, ohmically heated tokamaks barely achieve 2.5 keV.

Figure 4 also presents results with the fusion power included. Assumptions are comparable to those used for the tokamak studies. Ignition points, defined by the point where constant-density and constant-current positive temperature perturbations result in thermal runaway to a fusion dominated regime, are denoted by "x" in Fig 4a. Ignition at a current as low

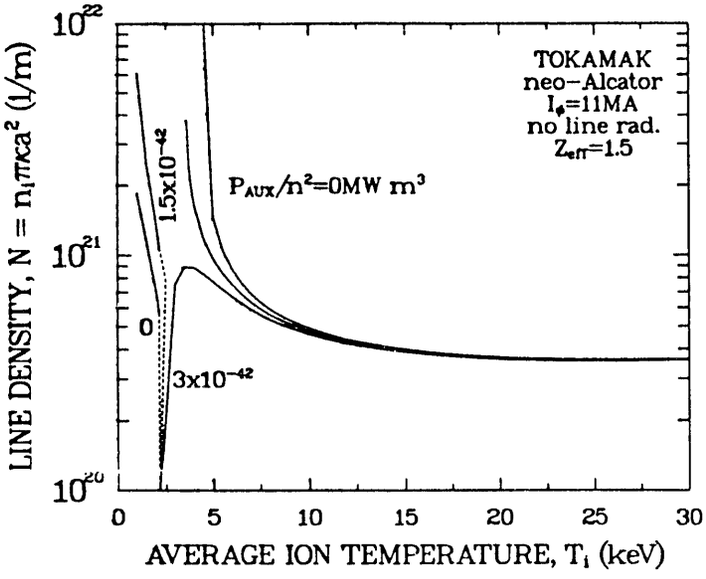

Fig. 2 Line density *versus* ion temperature steady-state operating points for a tokamak with neo-Alcator transport, no line radiation (but $Z_{eff} = 1.5$), and for the CIT-like assumptions.

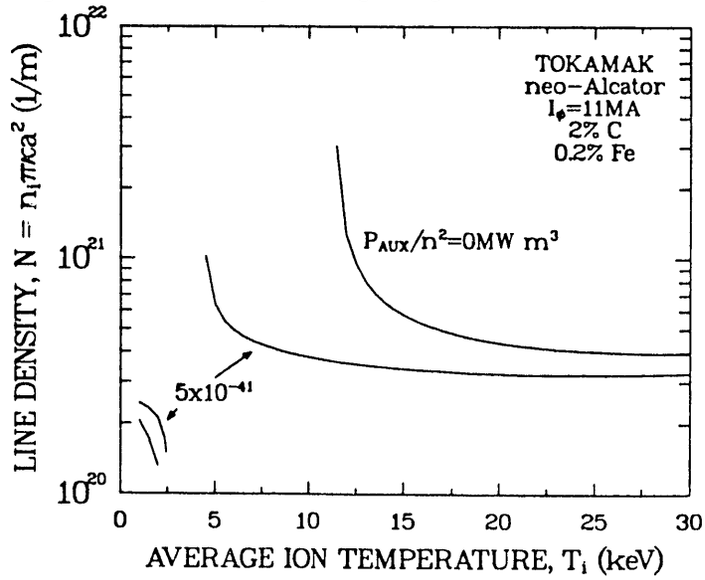

Fig. 3 Line density *versus* ion temperature steady-state operating points for a tokamak with neo-Alcator transport, 2% carbon and 0.2% iron, and the CIT-like assumptions.

as 8.1 MA is predicted using the basecase scaling assumption. The sensitivity of this ignition current to various assumptions is discussed in Sec. 3.4. The present results assume 2% C and 0.2% Fe impurity levels.

The ignition physics of the RFP and tokamak are significantly different. First, as previously discussed, the RFP has strong ohmic heating (100 times larger). Secondly, the transport scalings have an opposite dependence on density. For the tokamak this results in the ignited regime lying above an N *versus* T_i curve, as shown in Fig. 2. At higher density, major disruptions set an abrupt limit for tokamaks. For the RFP, Connor-Taylor confinement degrades weakly with density [see Eq. (6)], so that the ignited regime lies below the N *versus* T_i curve, as illustrated by the 12 MA case of Fig. 4a. No major disruption has been observed in the RFP. At lower density, however, the RFP must operate above electron runaway limits associated with a high streaming parameter. Ignition and reactor operating points will have streaming parameters below that of existing RFP experiments. Tokamak confinement scaling restricts the density to sufficiently high values that electron runaway (other than during disruptions) is generally not an issue.

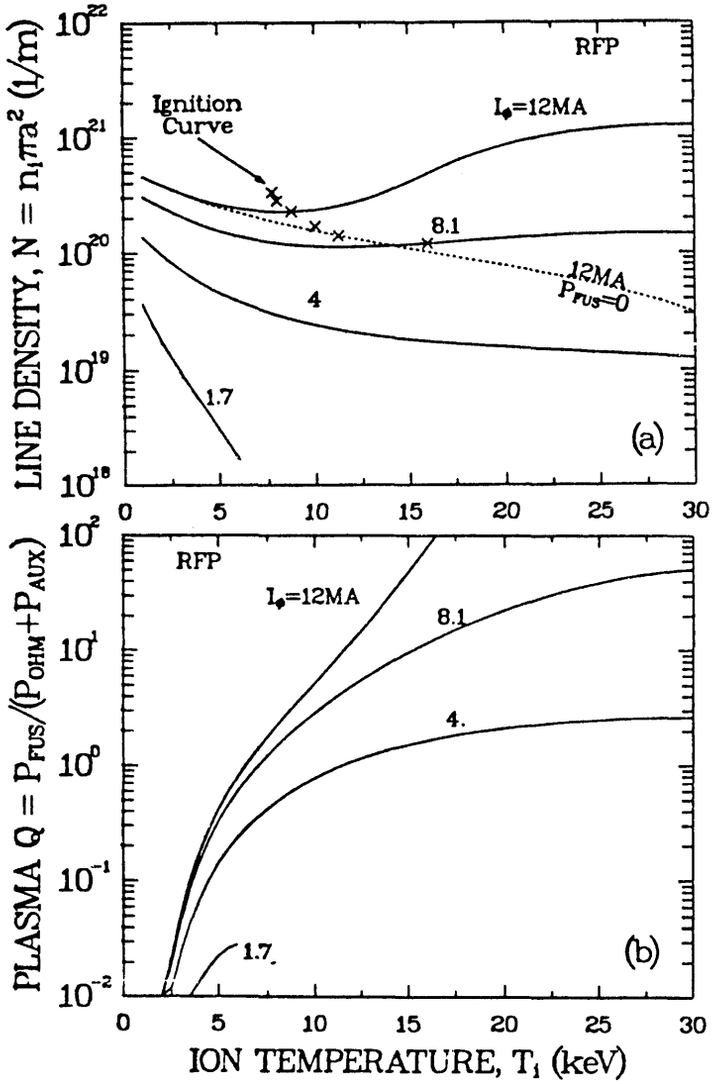

Fig. 4a Line density and (4b) Plasma Q, *versus* ion temperature in contours of constant plasma current for an RFP. In Fig. (4a), ignition points are marked with an "X", and the dashed curve represents a 12MA RFP with no fusion power.

A third difference is that tokamak ignition requirements are much more strongly affected than the RFP by impurity contamination. A relatively high concentration of low-Z impurity primarily affects plasma performance through an increased Z_{eff}, while a low concentration of high-Z impurity primarily causes significant line radiation. Both line radiation and Z_{eff} adversely impact tokamak energy balance. For the RFP, the effect is less dramatic since the already important ohmic heating term increases with Z_{eff}, so the extra source helps to balance the increased loss. The impurity concentrations assumed here result in $Z_{eff} \simeq 2.5$, compared to the CIT design assumption of $Z_{eff} = 1.5$. With these impurity levels, the RFP ignites at 8.1 MA, while CIT would not ignite for the design values of $I_\phi = 11MA$ and $P_{AUX} = 30\ MW$.

A fourth major difference between tokamak and RFP ignition physics is the tokamak requirement for auxiliary heating and the observation that auxiliary heating degrades confinement. While this effect makes ignition more difficult, it helps, once ignition is achieved, by limiting thermal runaway to lower temperatures (~40 keV) where fusion power is balanced by transport losses. This assumes that fusion-product heating will also degrade confinement. Ohmic heating in the RFP is so strong that auxiliary power is unnecessary, thus there exists no evidence that fusion heating ("auxiliary" heating) will degrade confinement. Present RFP confinement relations do not degrade with fusion power.

Operating-point burn control would also behave differently if fusion power did not degrade confinement. Tokamaks have a major disruption beta-limit constraint, such that thermal runaway (which may occur when the ignition boundary is crossed) could exceed this limit and destroy the plasma. The RFP has not exhibited disruptions, but has exhibited a "soft-beta" limit[16], where confinement is degraded. Such a limit would eliminate burn-control concerns in the RFP by expanding significantly the space of stable operating points.

Figure 4b shows that high-Q operation should be achievable and will be a function of the plasma current and beta. Because the ohmic heating is large in the RFP, plasma Q values will be lower than for an ignited tokamak with $P_{AUX} = 0$.

3.4. RFP Ignition-Current Sensitivity.

Using the Connor-Taylor basecase scaling law, the minimum current for ignition is 8.1MA. A parametric variation of the assumptions was performed to identify those that most strongly affect the ignition current. The profile factors, scaling law, cyclotron wall reflectivity, τ_{E_i}/τ_{E_e}, and impurity level were varied. The ignition current was found to be a strong function of five parameters, including the ion density profile, the carbon impurity level (Z_{eff}), the iron impurity level (P_{line}), and the coefficient (C_x) and exponent (X) of the transport scaling correlation [Eq. (6)]. Peaked density profiles increase the fusion reactivity in the plasma core and reduce the line radiation from the edge, resulting in a 2MA difference in the ignition current per 100% change in the ion density exponent $\alpha_n = 1$. Both Z_{eff} and P_{line} also affect the ignition current strongly, resulting in 1.5MA per 100% change in either iron or carbon impurity level. Significant reductions in the ignition current can be obtained by maintaining clean plasmas. The strongest variation of the ignition current is caused by uncertainties in the transport scaling. Both variations in the coefficient and the exponent (extrapolation distance is large) are important, changing the ignition current by ~1MA per $\Delta C_x = 1$ and ~2MA per $\Delta X = 0.1$.

A multi-parameter variation was performed to identify the best and worst ignition cases, and the results are summarized

in Table I. The basecase ignites at 8.1 MA. The "best" case uses a theoretical scaling ($X = 1$) benchmarked to ZT-40M ($C_\epsilon = 4.40$), has no impurities, and has a strongly peaked density profile ($\alpha_n = 2.5$). The "best" case ignites at 4.6 MA.

While the confinement scaling law with X = 1 has some theoretical justification, an arbitrary two-parameter fit to the international RFP database was made using the form of Eq. (6). The resulting fit has $X = 0.91$ and $C_\epsilon = 2.32$. This two-parameter fit was taken as a pessimistic scaling case, and it results in an ignition current of 12.0 MA. It is interesting to note that the theoretical scaling of Connor-Taylor falls well within the 95% confidence level of the two parameter fit. The ignition currents associated with the 95% confidence extrema result in ignition currents of 2.6 MA and 81 MA. While these extrema are probably meaningless, this exercise demonstrates the large uncertainty associated with extrapolating the present scaling correlation to ignition conditions. Clearly, a most pressing need in the RFP program is to extend, test, and improve the accuracy of the RFP transport scaling law.

TABLE I. RFP IGNITION CURRENT

Case	Transport Scaling		Impurity Fractions		Density Profile	Ignition Current
	C_ϵ	X	f_{Fe}	f_C	α_n	$I_\phi(MA)$
Best	4.40	1.00	0.0	0.0	2.5	4.6
Base	3.28	1.00	0.002	0.02	1.0	8.1
2-param.	2.32	0.91	0.002	0.02	1.0	12.0

4. SUMMARY AND CONCLUSIONS

A steady-state, O-D (profile-averaged) model was applied to describe two-temperature plasma power balance equations. The model is applicable to both tokamak and RFP, with appropriate differences in equilibrium, beta, ohmic heating, and transport energy confinement scaling for the two confinement concepts. The model need not specify confinement, but rather, can specify a beta constraint and then calculate particle fractions and the $n\tau_E$ required to achieve a steady state operating point. If in addition, transport losses (through an $n\tau_E$ scaling) are specified then N *versus* T_i actual operating points can be calculated.

First, the model was applied to both the tokamak and RFP to demonstrate that $n\tau_E$ ignition requirements are similar for both devices. The model was then used to study tokamak and RFP ignition conditions. The CIT design conditions using optimistic (neo-Alcator) and pessimistic (Goldston-H) were considered. For the optimistic case, a $11MA$ CIT would ignite with $12.5MW$ of auxiliary power if no impurities were present. If 2% C and 0.2% Fe were present, however, even the optimistic scaling case could not ignite at $11MA$, unless $P_{AUX} \geq 50MW$. Great care must be taken to minimize impurities, particularly high-Z impurities, in CIT. The pessimistic scaling case does not ignite at $11MA$, even without impurities.

For the RFP, the basecase ignition current is 8.1MA, with an optimistic-to-pessimistic range of 4.6-12 MA. Basecase RFP ignition point conditions are summarized in Ref. [4]. In addition to a lower ignition current than CIT, the RFP basecase also requires an aB product that is lower by a factor of 3. The ignition RFP, compared to a tokamak, has many physics advantages, including ohmic heating to ignition (no need for auxiliary heating systems), higher beta, lower ignition current, less sensitivity of ignition requirements to impurity effects, no hard disruptions (associated with beta or density limits), and successful operation with high radiation fractions ($f_{RAD} \sim 0.95$)[16]. These physics advantages, coupled with important engineering advantages associated with lower external magnetic fields, larger aspect ratios and smaller plasma cross sections translate into significant cost reductions[7] for both ignition and reactor applications. The primary drawback of the RFP is the uncertainty that the present scaling will extrapolate to reactor regimes. (There is no expectation that it should not.) The 4MA ZTH was expected to extend the $n\tau_E$ transport scaling data three orders of magnitude above ZT-40M results, and, if the present scaling held, to achieve a DT-equivalent scientific energy breakeven, $Q = 1$.

REFERENCES

[1] J. D. Lawson, "Reversed Field Pinch Reactor Study; I. Physical Principles," CLM-R-171, Culham Laboratory, England (1977).

[2] R. Hancox, R. A. Krakowski, and W. R. Spears, *Nucl. Engr. and Des.* **63** (1981) 251.

[3] K. A. Werley, "Reversed Field Pinch Ignition Requirements," *Nucl. Fusion* **31** (1991) 567.

[4] K. A. Werley, "Reversed Field Pinch Ignition Physics," Los Alamos National Lab. report LA-UR-89-4093 (1989).

[5] L. Spitzer, Jr., Physics of Fully Ionized Gases, Interscience, New York (1962).

[6] R. J. Goldston, "Energy Confinement Scaling in Tokamaks: Some Implications of Recent Experiments with Ohmic and Strong Auxiliary Heating," *Plasma Physics and Controlled Nucl. Fusion* **26** (1984) 87.

[7] C. G. Bathke, R. A. Krakowski, R. L. Miller, and K. A. Werley, "ZTI: Preliminary Characterization of an Ignition Class Reversed-Field Pinch," *Fusion Tech.* **19** (1991) 1076.

[8] J. N. DiMarco, "Update of RFP Scaling Data," Los Alamos National Laboratory Report LA-UR-Revised-88-3375 (1988).

[9] J. W. Connor and J. B. Taylor, "Resistive Fluid Turbulence and Energy Confinement," *Phys. Fluids* **27** (1984) 2676.

[10] F. Troyon, R. Graber, H. Saurenmann, S. Semenzato, and S. Succi, *Plasma Phys. and Controlled Fus.* **26** (1984) 209.

[11] J. Galamobs and Y-K. M. Peng, "Ignition Criterion for $D-^3He$ Tokamak and Spherical Torus Reactors," to be published in *Fus. Tech.*

[12] N. A. Uckan, J. S. Tolliver, W. A. Houlberg, and S. E. Attenberger, "Influence of Fast Alpha Diffusion and Thermal Alpha Buildup on Tokamak Reactor Performance," *Fus. Tech.* **13** (1988) 411.

[13] J. A. Schmidt and H. P. Furth, "Compact Ignition Tokamak (CIT) Conceptual Design Report," A-860606-P-01 Princeton Plasma Physics Lab., Princeton, NJ (June 6, 1986).

[14] E. A. Chaniotakis, J. P. Freidberg and D. R. Cohn, "CIT Burn Control using Auxiliary Power Modulation," IEEE 13th Symposium on Fusion Engineering, Knoxville, TN, Vol. 1 (Oct. 1989) 400.

[15] P. Thullen, K. F. Schoenberg, D. Baker et al., "ZT-H Reversed Field Pinch Experiment Technical Proposal, " Los Alamos National Lab. report LA-UR-84-2602 (1984).

[16] M. M. Pickrell, J. A. Phillips, C. P. Munson, P. G. Weber, G. Miller, K. F. Schoenberg, and J. C. Ingraham, *16th European Conf. on Controlled Fus. and Plasma Phys.*, Venice, European Phys. Soc., Vol. II (March 1989) 749.

END

DATE FILMED

12/10/91